Thermal Environment Around the Space Shuttle with Hot-Gas Jets for Ice Suppression

A. K. Singhal* and L. T. Tam†
CHAM of North America Inc., Huntsville, Alabama
and
F. Bachtel‡ and J. Vaniman§
NASA Marshall Space Flight Center, Huntsville, Alabama

To prevent prelaunch ice formation on the external tank of the Space Shuttle, the final selected approach is to heat the surrounding air with vertical hot-gas jets located at the launch pad. This approach was considerably more cost-effective than other ice suppression methods considered, although its feasibility was not easily discernible due to the complex flowfield interactions. This paper describes how the use of vertical jets was first evaluated with the aid of a computational fluid dynamics (CFD) technique. An existing general-purpose CFD program (PHOENICS) was used to predict the thermal environment around the Shuttle under various jet configurations and wind conditions. The program accounts for effects of buoyancy, turbulence, and structural obstructions in the flowfield. The computed results showed physically plausible and consistent trends. The wind wake effects were found to be significant, and normally resulted in higher temperatures on the leeward side of the tank. High wind conditions were found to be more severe than calm wind conditions. The use of four jets with two different temperatures was identified as a promising option in which the air temperatures were raised sufficiently to prevent ice formation on the external tank, without excessive increase in Orbiter surface temperature. The use of the numerical model also facilitated the selection of test configurations and a test matrix for verifying the approach. Selected results of an experimental verification (by using a 2% scale model in a wind tunnel) are also presented.

Nomenclature

C	= turbulence model constant
g	= gravity acceleration
G	= turbulence generation term
IX,IY,IZ	= calculation domain
k	= turbulence kinetic energy
u	= velocity
x	= coordinate distance
δT	= temperature above ambient
σ	= Prandtl/Schmidt number
ϵ	= dissipation rate of turbulence kinetic energy
μ	= viscosity
ρ	= density

Subscripts

$1,2,D,\epsilon,k$	= turbulence model constants
B	= buoyancy
i,j	= coordinate directions
t	= turbulence

Introduction

FOR the practical use of the Space Shuttle, it is desirable that the Shuttle can be launched in all weather conditions. During cold weather, ice can form on the external tank (ET) after it is loaded with liquid hydrogen and oxygen. These ice formations would tend to break up during launch, and could damage the ceramic tiles on the underside of the Orbiter. To prevent ice formation, one of the solutions NASA studied in 1981 was to use the heat of jet engine exhaust gases. This method of heating the air could also reduce the amount and cost of the insulation required on the ET.

Initially, horizontal jets were planned for use. However, this would have required a vertical support tower, which had to be built specially for this purpose. A more attractive alternative was to use vertical jets, emerging from the launch pad. The purpose of the numerical modeling study was to examine the adequacy of the vertical-jets approach.

Numerical analyses of the thermal environment around the Space Shuttle under various wind conditions were carried out to examine the relative effectiveness of various feasible jet locations and conditions. Numerical modeling provided a quick and economical evaluation of the feasibility of using jets on the launch pad. It also provided three-dimensional distributions of air velocity, pressure, and temperatures, which were useful for: 1) better understanding of the interactions of winds, jets, and Space Shuttle components, 2) identification of the worst wind conditions, and 3) selection of suitable jet parameters.

This paper presents the salient features of the numerical model, selected test-case studies of full-scale simulation used to establish the feasibility of the vertical-jets approach, and selected results of small-scale simulation used for verification against wind-tunnel experiments.

The present study was performed in 1981-1982 (Final Reports: Refs. 1 and 2); since then the approach has been verified further and has already been tested and implemented at a launch site.

Numerical Model

An existing general-purpose computational fluid dynamics program, PHOENICS, was employed for numerical simula-

Received May 21, 1985; revision received Dec. 2, 1985.

*President and Technical Director.
†Senior Engineer.
‡Aerospace Engineer, Thermal Engineering Branch (EP44).
§Chief, Space Station Systems Division (EL81).

tions of selected test cases. PHOENICS[3,4] has the necessary flexibility to represent solid obstacles of arbitrary shapes, and had previously been applied to problems of similar complexity[5,6] with favorable results. PHOENICS provides simultaneous solutions of governing transport equations by employing a fully conservative, finite domain (or control volume) approach with the use of staggered-grid and hybrid-differencing practices.[7]

The salient features of the numerical model constructed for the present study are summarized below.

1) The flow is treated as steady, three-dimensional, turbulent, and elliptic. Figure 1 shows a sample calculation domain and grid distribution. The calculation domain is subdivided into 4224 control cells with highly nonuniform grid distributions in each coordinate direction. This grid distribution permits good resolution of the solution in the area of interest, i.e., near the tank surface. All flow variables [pressure, enthalpy, three velocity components, and two turbulent quantities (k, ϵ)] are calculated at all control cells.

2) The jet positions, exit temperature, and mass flow rates are prescribed as input conditions. Similarly, the magnitude and direction of the wind are specified as boundary conditions at the upwind face of the calculation domain. Wind speed is assumed to vary linearly with vertical distance from the launch pad.

3) Solid objects such as the external tank, boosters, and Orbiter are represented by way of local "porosities." The variable porosity or blockage concept has been used successfully in many other applications.[5-8] Separate values of porosity are assigned to the cell-volume and cell-face areas. Volume porosity of a cell is defined as the ratio of the volume accessible to the fluid to the total volume of the control cell. All porosity values, therefore, lie in the range of 0-1.

4) The top, side, and downstream boundaries of the calculation domain are treated as free or constant-pressure boundaries; i.e., fluid is allowed to enter or exit depending on the local calculated difference between the near-boundary grid pressure and the ambient pressure.

5) The bottom plane of the calculation domain, which is aligned with the top of the launch pad, is treated as an impervious surface.

6) The exit hot gases of the vertical jets are considered to be inert.

7) Buoyancy effects are taken into account by having an appropriate gravity force term in the vertical-direction momentum-conservation equation.

8) Turbulence effects are accounted for by using a two-equation ($k\sim\epsilon$) turbulence model,[9,10] which is the model most commonly used for complex flows and represents a state-of-the-art technique for engineering applications. In the $k\sim\epsilon$ model, the local state of turbulence is characterized by two scalar quantities, viz., turbulence kinetic energy k and its dissipation rate ϵ. The local turbulent or eddy viscosity μ_t is computed from k and ϵ as follows:

$$\mu_t = \rho C_D k^2/\epsilon \tag{1}$$

where ρ is fluid density and C_D an empirical constant.[10] Both k and ϵ are calculated from transport equations. In the present work, due to the importance of buoyancy, the following modified $k\sim\epsilon$ equations are employed:

$$\rho\frac{Dk}{Dt} = \frac{\partial}{\partial x_i}\left(\frac{\mu_t}{\sigma_k}\frac{\partial k}{\partial x_i}\right) + G_k - \rho\epsilon + G_B \tag{2}$$

$$\rho\frac{D\epsilon}{Dt} = \frac{\partial}{\partial x_i}\left(\frac{\mu_t}{\sigma_\epsilon}\frac{\partial \epsilon}{\partial x_i}\right) + \frac{\epsilon}{k}(C_1 G_k - C_2\rho\epsilon + C_1 G_B) \tag{3}$$

where

$$G_k = \mu_t\left(\frac{\partial u_i}{\partial x_j} + \frac{\partial u_j}{\partial x_i}\right)\frac{\partial u_j}{\partial x_i}$$

and

$$G_B = \frac{\mu_t}{\rho} g_i \frac{\partial \rho}{\partial x_i}$$

The term G_B represents generation/suppression of turbulence due to buoyancy.[11] The empirical constants used in the calculations are those recommended in the original references[10,11]: $C_1 = 1.44$; $C_2 = 1.92$; $C_D = 0.09$; $\sigma_k = 1.0$; and $\sigma_\epsilon = 1.3$.

9) All solid surfaces (surfaces of the launch pad, ET, booster, and Orbiter) are treated as inviscid and impervious; i.e., skin friction losses are neglected in the momentum equation. This simplification was made for convenience and was not considered to be critical for the first stage of the relative evaluation studies.

10) All solid surfaces are also treated as adiabatic. This assumption is made in view of the following: a) The gas temperatures are not expected to be significantly affected by the heat loss or gain to solids; b) the surface temperatures of solids can be calculated separately at the desired positions from the predicted velocity and temperature distributions.

Feasibility and Optimization Study

This study was carried out in five stages in a building-block manner. In the first two stages, simplified configurations were used to quickly establish the adequacies of the selected CFD technique and of the vertical-jets approach of ice suppression. In the last three stages, Space Shuttle geometry was included in the numerical model. Selected test cases and results of each stage are briefly described below, with main emphasis on stage 4. Computational details (solution convergence characteristics and computer time requirements) are also given at the end of this section.

In the first stage, a single jet was initially considered with cross winds of different speeds. Then a vertical rectangular column of the size of the external tank was introduced first on the windward side and then on the leeward side. The results of

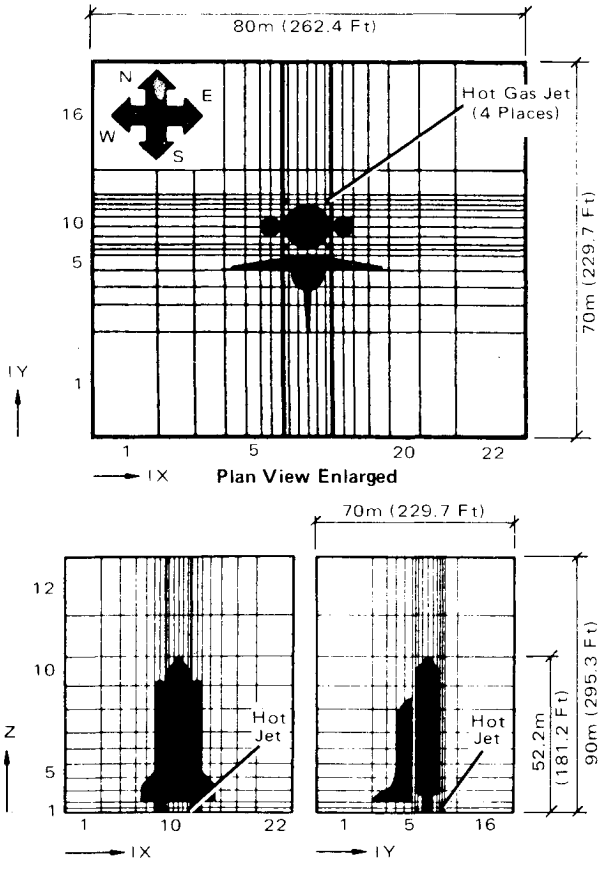

Fig. 1 Computational grid and relative positions of Shuttle components and hot-gas jets.

these cases clearly showed the wake effects; i.e., a jet on the leeward side tends to cling to the column and provides more effective air heating (Figs. 2a and 2b). This finding was important because the leeward side of the external tank is most susceptible to icing because the convective heat transfer tends to be high on the windward side.

In the second stage of the study, different combinations of jet velocity and temperature were simulated to determine a set of conditions that would sufficiently raise air temperatures near the top without generating excessively high temperatures near the bottom of the column. This was done in anticipation of the operational restrictions on maximum permissible temperature near the Orbiter. Figure 2c shows the result of a case with higher jet velocity and lower temperature. The comparison of Figs. 2b and 2c confirms the expectation of more effective heating with higher jet velocity and lower temperature. Results of other parameters studied (e.g., distance between the jet and column, and multiple jets) are reported in Ref. 1.

In the third stage, the rectangular column was replaced by the Space Shuttle geometry. Calculations were performed for normal winds, i.e., from the straight front or behind the Orbiter. Due to the symmetry, only one-half of the Shuttle was considered. This permitted an economical assessment of the effects of three different wind speeds: calm wind, 3-5 knots; mild wind, 6-8 knots; and strong wind, 20-22.8 knots. Figure 3 shows comparisons of velocity and temperature fields near the top of the external tank for the calm wind and strong wind cases.

In the fourth stage, the full Space Shuttle was simulated to evaluate the effects of wind direction. Five test cases were considered to simulate five different wind directions (designated as N, S, E, NE, and SE). In all five cases, jet diameter = 3 ft (0.9 m), jet temperature = 500°F (260°C), and jet velocity = 750 ft/s (228.6 m/s). Salient features of stage 4 results are illustrated in Figs. 4-8 and discussed below.

Cases 1-5

Air-Temperature Variations

Figure 4 shows the predicted air temperatures for case 1 (northward wind, from behind the Orbiter). It presents temperature variations in the vertical direction, in the vicinity of the external tank, at eight different angular locations marked 1-8 in the plan view. In the same diagram, the maximum temperature along the Orbiter surface, varying with the vertical elevation, is shown by the dotted line. A similar diagram for case 3 (side wind) is presented in Fig. 5.

Figure 6 shows, for test cases 1-5, isotherms of 10, 20, and 40°F (5.6, 11.1, and 22.2°C) above ambient at three horizontal planes, viz.: $IZ = 4$, 9, and 10 passing through 34.1, 134.2,

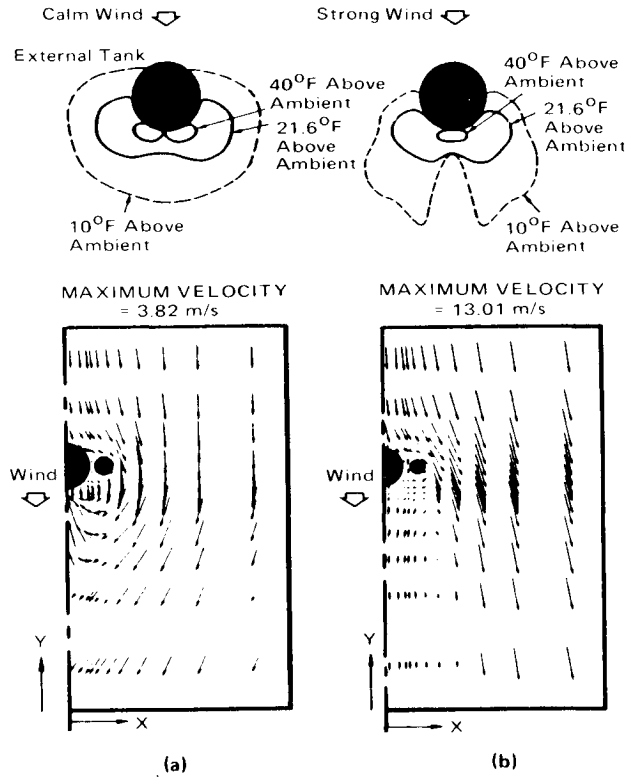

Fig. 3 Temperature and velocity distributions near the top of the Space Shuttle's external tank (at $IZ = 10$ and 9, respectively, Fig. 1) for: a) calm wind (3-5 knots), and b) strong wind (20-22.8 knots).

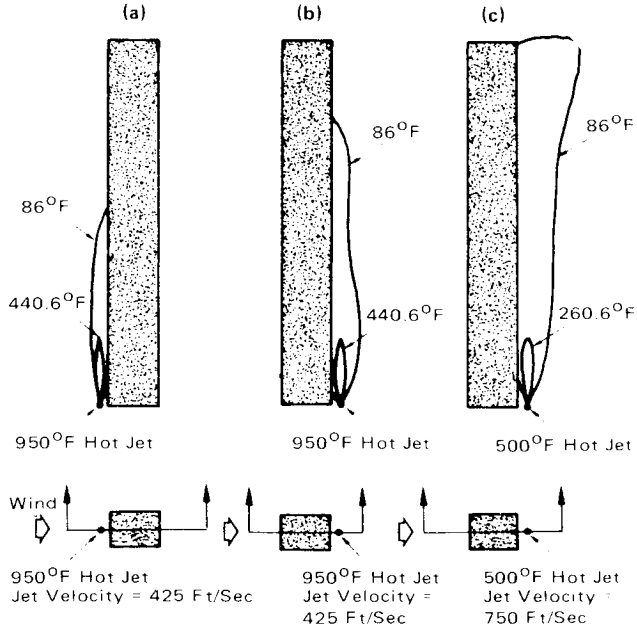

Fig. 2 Temperature contours of a single vertical hot jet located on the windward and leeward sides of a rectangular column: a) jet on the windward side; b) jet on the leeward side; and c) jet on the leeward side with higher jet velocity and lower temperature.

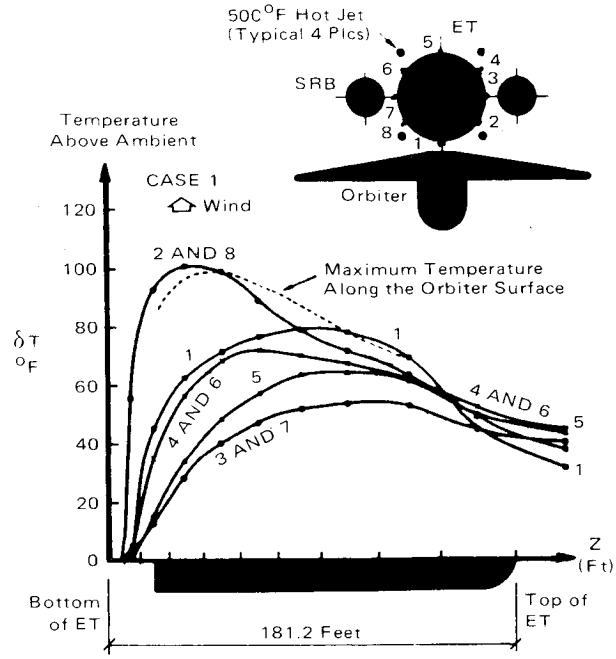

Fig. 4 Variation of air temperature along the external tank at several circumferential positions, and along the Orbiter; case 1.

and 164.4 ft (10.4, 40.9, and 50.1 m), respectively, from the launch pad.

From Figs. 4-6, the following points may be noted.

1) For case 1, the results are symmetrical about the vertical plane ($IX = 11$). This symmetry is consistent with the imposed boundary conditions, and confirms that the calculation scheme does preserve symmetrical conditions where applicable.

2) The northward wind (case 1) results show the best thermal environment; i.e., as compared to cases 2 and 3, the temperatures near the top of the external tank are higher, and the peak temperatures near the lower part of the Orbiter are lower.

3) Cases 1 and 2 show general trends similar to those predicted for earlier test cases[1]; i.e., more effective heating takes place on the leeward side of the tank. The peak temperature is about 100°F (55.6°C) above ambient (see Fig. 4).

4) Case 3 (eastward wind) shows the poorest heating as compared to cases 1, 2, 4, and 5. For instance, Fig. 5 shows that at angular positions 6 and 7, temperature rises near the top of the external tank are less than 10°F (5.5°C), while the peak temperatures are more than 120°F (66.7°C) above ambient.

5) Cases 4 and 5 show the temperature contours consistent with other cases. In these cases, too, the wake effects are noticeable (see Fig. 6).

Velocity Distribution

Figure 7 shows velocity distributions for test cases 1-5 in the $IZ = 9$ horizontal plane. Figure 8 shows the velocity distributions in selected horizontal and vertical planes for test case 1. The main observations from the velocity-vector diagrams are:

1) Effects of change in wind direction shown in Fig. 7 are physically plausible.

2) For case 1, the velocity fields are, as expected, symmetric about the midvertical plane (see Fig. 8).

3) The positions of the ET, solid rocket booster (SRB), and Orbiter can be identified in velocity diagrams by observing the blank areas.

4) Figure 8 also shows the velocity vectors at a windward plane, in front of the Orbiter (see Fig. 1 to locate the plane $IY = 3$). The downward motion is a consequence of the wind hitting the Orbiter and being deflected in all four directions, as well as of the suction effect produced by the hot jets on the launch pad.

5) Inspection of Fig. 8 for case 1 reveals that the overall flow patterns are physically plausible; i.e., the flow turning, acceleration, and flow reversal due to various solid objects (ET, SRB, and Orbiter) and due to the wind conditions are in conformity with the commonly observed basic hydrodynamic characteristics.

Test Cases of Stage 5

In the fifth and final stage of the numerical study, five additional test cases (6-10) were devised to further optimize the jet parameters. All conditions were as in cases 1-5, except for reductions in exit gas temperature and velocity of the two jets closest to the Orbiter. These changes were to satisfy anticipated velocity and temperature constraints at the vehicle. The exit gas temperature of the two jets was reduced from 500 to 300°F (260 to 148.9°C). The exit gas velocity for the same two jets was reduced from 750 to 675 ft/s (228.6 to 205.7 m/s). (The jet exit conditions selected after subscale and initial full-scale testing were an exit temperature of 250°F and an exit velocity of 550 ft/s, just slightly less than those used in the final stage of numerical modeling study.) The selected wind conditions for each case were as follows: Cases 6, 7, and 8 had easterly winds of 6-8, 3-5, and 12-15 knots (3.1-4.1, 1.55-2.58, and 6.18-7.73 m/s), respectively, and cases 8 and 9 had northeasterly winds of 6-8 and 12-15 knots (3.1-4.1 and 6.18-7.73 m/s), respectively.

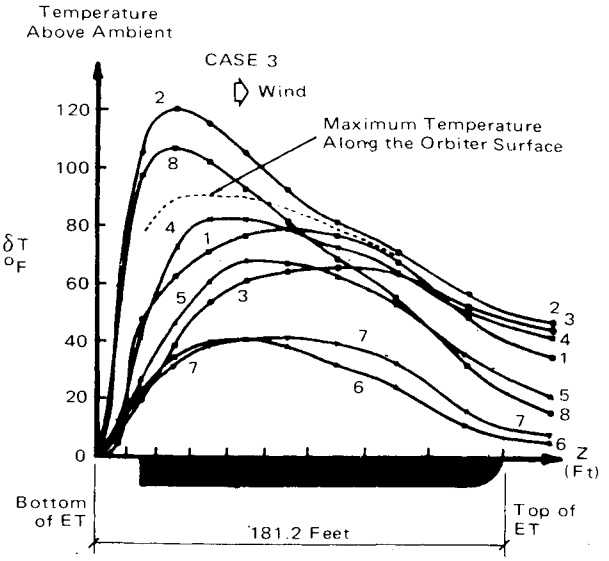

Fig. 5 Variations of air temperature along the external tank at several circumferential positions, and along the orbiter; case 3.

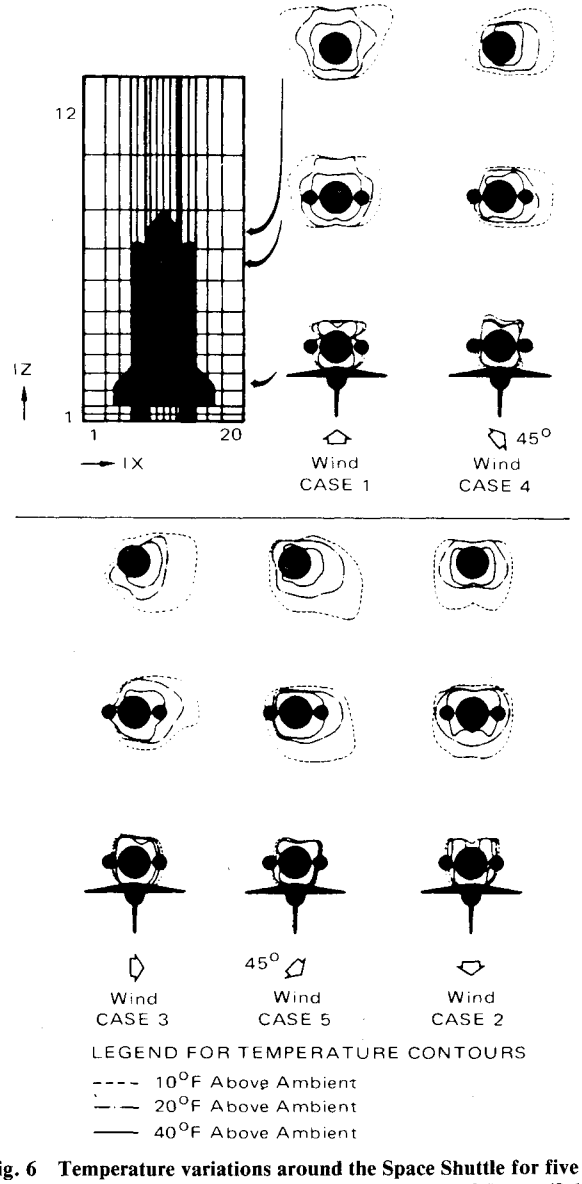

Fig. 6 Temperature variations around the Space Shuttle for five different wind directions (cases 1-5); wind velocity = 6-8 knots (3.1-4.1 m/s), linear variation with elevation.

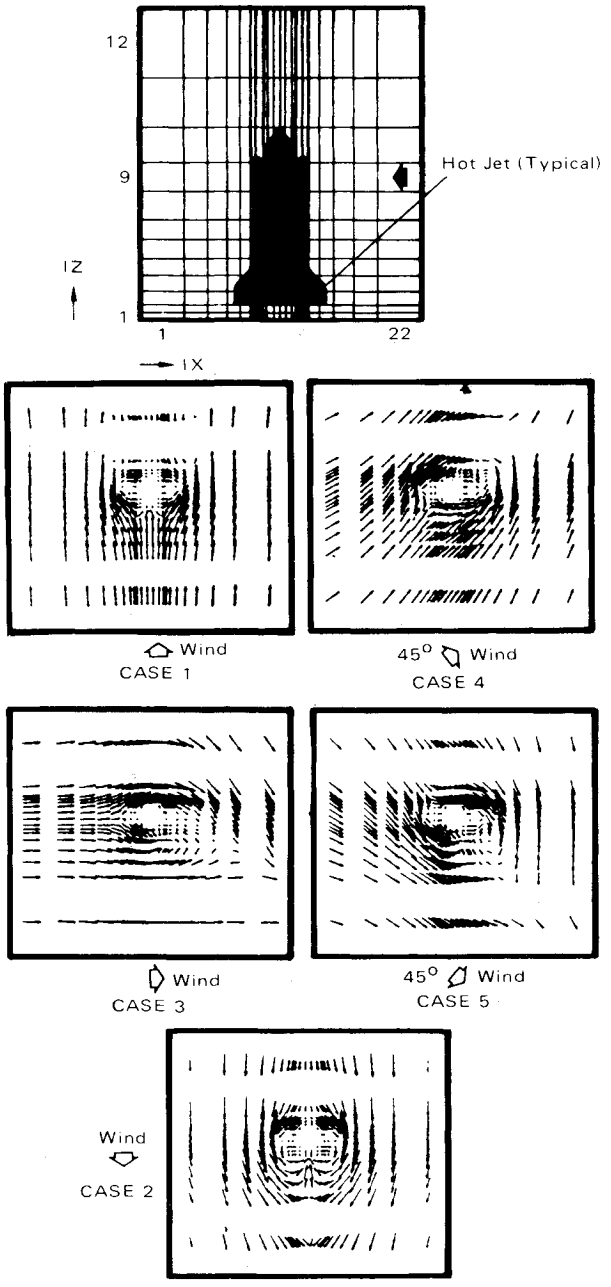

Fig. 7 Velocity distributions in a horizontal plane ($IZ = 9$), under different wind directions, cases 1-5; wind velocity = 6-8 knots.

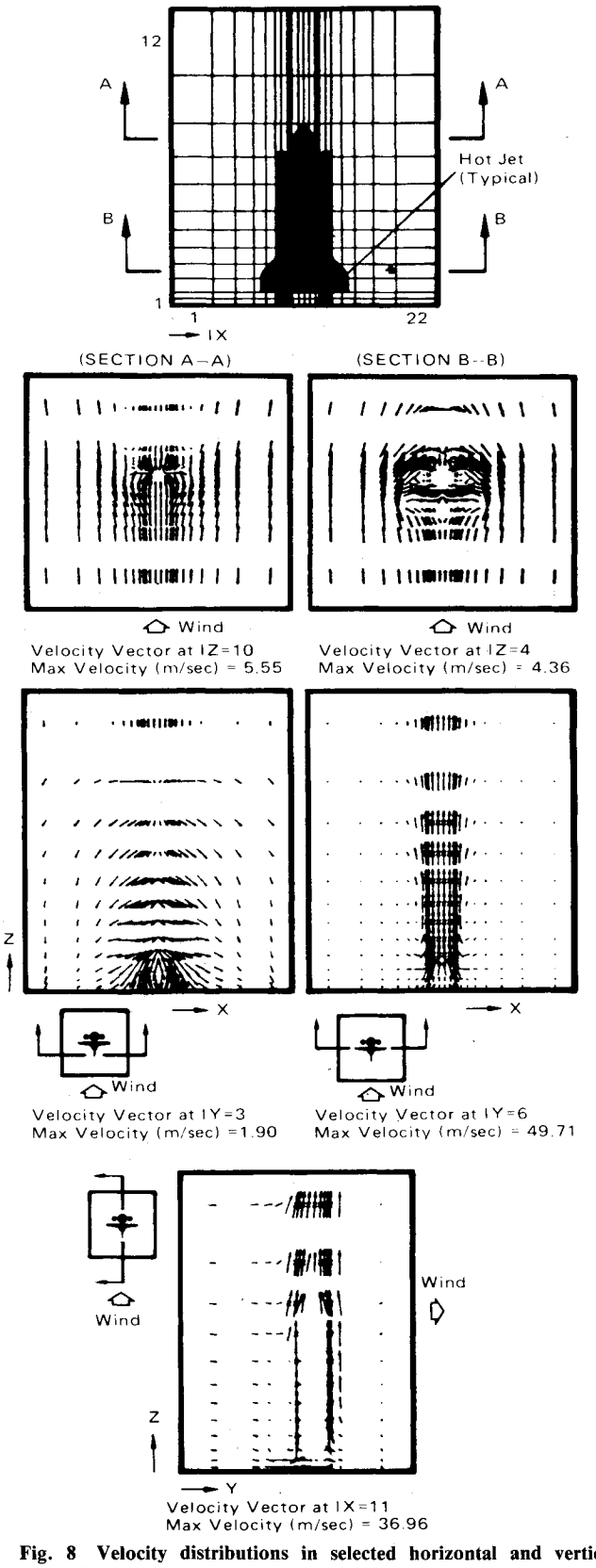

Fig. 8 Velocity distributions in selected horizontal and vertical planes for test case 1.

The calculated results of cases 6-10 revealed the following:

1) The jet conditions for cases 6-10 resulted in relatively better thermal environments than those seen from cases 1-5. The peak temperatures reduced from 120 to 80°F (66.7 to 44.4°C) above ambient.

2) The high eastward wind (case 8) shows the poorest heating as compared to all other test cases. However, due to the high wind velocity conditions, the convective heat transfer will be high in the regions of lowest temperatures (i.e., on the windward side of the tank) and, therefore, the external tank icing potential is not as poor as it may seem from the temperatures alone.

Computational Details

Satisfactory results for all of the test cases were obtained without any numerical computational problems. All solutions were well converged within 150 sweeps (iterations); i.e., all error residuals were reduced by at least two orders of magnitude, and all flow variables settled within 1%. Computer time requirements were modest; for example, 180 seconds CPU time on a CRAY-1 computer were required for each case with 4224 control cells employed.

Verification Study

The numerical modeling study described previously established the feasibility of using vertical hot-gas jets for ice suppression, and was followed by an experimental verification

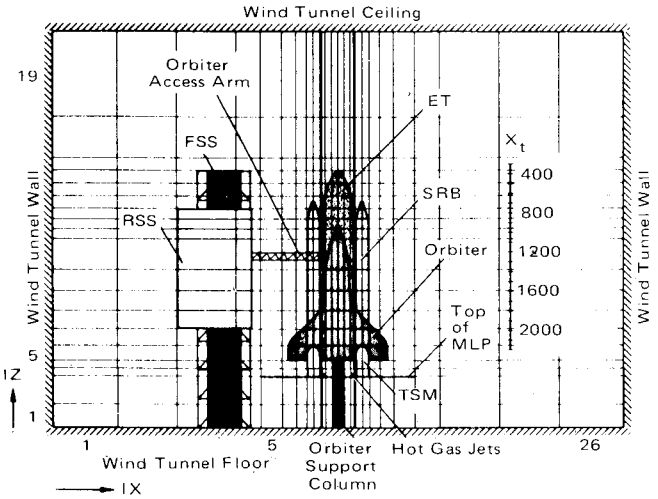

Fig. 9 Numerical model setup for 1.8% scale model wind-tunnel test.

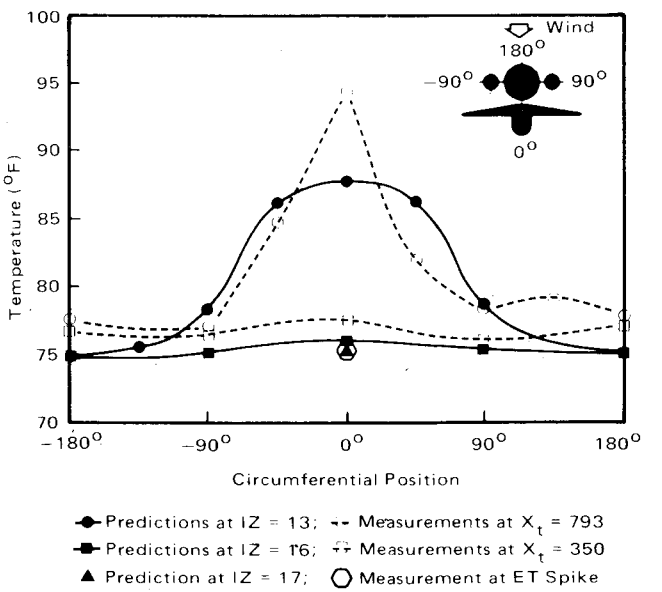

Fig. 10 Air temperatures around 1.8% scale model of the Space Shuttle.

study. A 1.8% scale model of the Space Shuttle was used, and five tests were conducted in a wind tunnel.[12] Measurements included temperatures at three elevations and mean flow velocities at selected positions. In parallel, the numerical model was set up for the planned tests.[2] Figure 9 presents a cross section of the scale model for the wind-tunnel tests, showing the Space Shuttle model, side support tower model, and selected grid distributions. In this numerical model, the side, top, and bottom boundaries of the calculation domain are solid surfaces (to represent the wind-tunnel walls), rather than free surfaces used in the full-scale simulation. A total of 8892 control cells were used with grid distributions similar to those used in the earlier study.

Figure 10 shows a comparison of measured and predicted air temperatures at three elevations, for a 20-knot (10.3 m/s) wind case with four jets of 514 ft/s (156.7 m/s) and 197°F (91.7°C), and the wind temperature of 75°F (23.9°C). The noteworthy points of this comparison are: 1) at the lower elevation ($IZ = 13$ in Fig. 9), the numerical model underpredicts the peak temperature by approximately 5°F; 2) at the higher elevation ($IZ = 16$) the agreement is much better; and 3) at the highest location (ET spike at $IZ = 17$), the agreement is excellent. The main reason for temperature underprediction at the lower elevation is the use of a coarse grid in computations, which is expected to smear the temperature and velocity profiles. Another possible contributing factor is the omission of wall friction in the numerical model. On the other hand, since the numerical method is fully conservative, agreement should, and does, improve with the downstream distance.

The measured velocities were not satisfactory because of high turbulence in the flow, and, therefore, velocities were not used for verification. Flow visualization did reveal general similarities between the predicted and observed flow patterns.

This study was followed up with an experimental investigation with a 10% scale model,[13] and finally with some on-site tests[14] with the ice suppression system commissioned for use in actual Space Shuttle launches.

Conclusions

1) The results of the feasibility study showed physically plausible trends, and clearly illustrated the relative effectiveness of the parameters considered. For example, the effects of changes in wind direction supported the approach of heating air by vertical jets located on the launch pad. These results also demonstrated the capability of the employed numerical technique and computer code.

2) Verifications of selected cases by small-scale wind-tunnel tests further supported the feasibility of using vertical jets for ice suppression.

3) In general, the present study demonstrates a practical application of the employed computational fluid dynamics technique.

Acknowledgments

This study was supported by the NASA Marshall Space Flight Center, under Contract NAS8-34352. The authors wish to acknowledge Drs. Laurence Keeton and Andrzej Przekwas of CHAM for many helpful discussions and suggestions. Thanks are due to Ms. Kelli King for preparing the typescript of this paper.

References

[1]Singhal, A. K. and Tam, L. T., "Numerical Analysis of Thermal Environment Around the Space Shuttle with Vertical Hot Gas Jets on Launch Pad," CHAM of North America Inc., Huntsville, AL, Rept. H3490/10, March 1982.

[2]Singhal, A. K. and Tam, L. T., "Numerical Modeling of Flow Around 2% Scale Model of Space Shuttle," CHAM of North America Inc., Huntsville, AL, Rept. H3591/1, Nov. 1982.

[3]Spalding, D. B., "A General Computer Program for Multi-Dimensional One- and Two-Phase Flows," *Mathematics and Computers in Simulation*, Vol. XXIII, North Holland Press, the Netherlands, 1981, pp. 267-276.

[4]Singhal, A. K., "A Critical Look at the Progress in Numerical Heat Transfer and Some Suggestions for Improvement," *Numerical Heat Transfer*, Vol. 8, Hemisphere Publishing Corp., Washington, DC, 1985, pp. 505-517.

[5]Planning Research Corporation, "Solid Rocket Motor/Vehicle Assembly Building Inadvertent Ignition Effects Study," NASA KSC-DF-441, Sept. 1981; also, "Solid Rocket Motor/Vehicle Assembly Building Inadvertent Ignition Effects Study Executive Summary," NASA KSC-DF-502, Sept. 1981.

[6]Markatos, N. C. and Mukerjee, T., "Three-Dimensional Computer Analysis of Flow and Combustion in Automative Internal Combustion Engines," *Mathematics and Computers in Simulation*, Vol. XXIII, No. 4, Dec. 1981, pp. 354-366.

[7]Patankar, S. V., "Numerical Heat Transfer and Fluid Flow," *Series in Computational Methods in Mechanics and Thermal Sciences*, McGraw-Hill Book Co., New York, 1980.

[8]Singhal, A. K. and Spalding, D. B., "Mathematical Modeling of Multi-Phase Flow and Heat Transfer in Steam Generators," *Multiphase Transport: Fundamentals, Reactor Safety Applications*, Vols. 1-5, Hemisphere Publishing Corp., Washington, DC, 1980, pp. 373-406.

[9]Harlow, F. H. and Nakayama, P. I., "Transport of Turbulence Energy Decay Rate," Los Alamos Science Lab, University of California, Rept. LA-3854, Feb. 1968.

[10]Launder, B. E. and Spalding, D. B., "The Numerical Computation of Turbulent Flows," *Computer Methods in Applied Mechanics and Engineering*, Vol. 3, 1974, pp. 269-289.

[11]Markatos, N. C., Malin, M. R., and Cox, G., "Mathematical Modeling of Buoyancy-Induced Smoke Flow in Enclosures," *International Journal of Heat Transfer*, Vol. 25, No. 1, 1982, pp. 63-75.

[12]Porteiro, J. L. F., Norton, D. G., and Pollock, T. C., "Space Shuttle Ice Suppression System Validation," Vols. I-II, Texas A&M, Rept. TEES-TR-4587-82-01.

[13]Schmitt, D. A., Heckel, G. W., and Seiderman, B., "Preliminary Analysis of Aerothermal Data from Subscale Tests of the VAFB Ice Suppression System for the Space Shuttle Vehicle," Martin Marietta Aerospace, Denver, CO, Rept. VCR-83-405, Sept. 1983.

[14]Schmitt, D. A. and Owens, L. E., "Data Analysis Report for the Facility Verification Vehicle Test of the Space Shuttle Ice Suppression System," Martin Marietta Aerospace, Denver, CO, Rept. VCR-85-486, July 1985.